JOURNAL OF MATERIALS SCIENCE 29 (1994) 262–268

Formation of plate-like lanthanum-β-Aluminate crystal in Ce-TZP matrix

M. MIURA, H. HONGOH, T. YOGO, S. HIRANO
Department of Applied Chemistry, School of Engineering, Nagoya University, Furo-cho, Chikusa-ku, Nagoya 464-01, Japan

T. FUJII
Technical Research Center, Nisshin Flour Milling Co., Ltd, 5-3-1 Tsurugaoka, Oi-machi, Iruma-gun, Saitama 354, Japan

The reaction route and morphology of lanthanum-β-aluminate (LBA) crystals formed in Ce-TZP matrix were studied by examining the crystal phase changes and the microstructures in relation to the heat-treatment time, heat-treatment temperatures and the particle size of raw Al_2O_3 powders. In the Ce-TZP matrix, the LBA crystal was formed by the reaction between La_2O_3 and Al_2O_3 through the $LaAlO_3$ phase as the intermediate. $La_2Zr_2O_7$ forms at 800 °C and remains in the temperature range 800–1500 °C, and $LaAlO_3$ forms between 1200 and 1400 °C. The $LaAlO_3$ reacts with Al_2O_3 to form LBA above 1500 °C. The diffusion of La^{3+} through the $La_2Zr_2O_7$ phase was faster than that of Al^{3+}. The morphology of LBA crystals was dependent on the particle size of the starting raw Al_2O_3 particle. When submicrometre size Al_2O_3 (0.4 μm) particles were used as the starting particles, anisotropic, plate-like LBA crystals, about 10 μm long, were formed during heat treatments. On the other hand, Al_2O_3 of larger grain sizes (3.6, 10.3 μm) yield conglomerates of LBA crystals. The size of the conglomerates is similar to that of the raw Al_2O_3 particle. The dependence of the morphology of LBA on the particle size of Al_2O_3 can be attributable to the sintering process of the Ce-TZP matrix, leading to the control of the mechanical properties of Ce-TZP ceramics with LBA crystals.

1. Introduction

Tetragonal ZrO_2 polycrystal (TZP) ceramics show excellent mechanical properties with high strength and fracture toughness. Although Y_2O_3 is known as an effective stabilizing agent for tetragonal zirconia, yttria-doped tetragonal zirconia (Y-TZP) is reduced in strength during low-temperature or hydrothermal ageing [1]. Ceria-doped tetragonal zirconia (Ce-TZP) is superior to Y-TZP [2, 3], which is widely used in the field of engineering ceramics, for fracture toughness and high stability against low-temperature degradation. However, the application of Ce-TZP is limited only to specific cases, because its fracture strength is about one-half that of Y-TZP ceramics. The dispersion of Al_2O_3 particles is known to be effective for increase of the fracture strength of Ce-TZP [4], but to decrease the fracture toughness. The authors found that the *in situ* formation of Ce-TZP/Al_2O_3/LBA (lanthanum-β-aluminate, $LaAl_{11}O_{18}$) composites during sintering could be a promising way to improve the fracture strength of Ce-TZP without reducing the high fracture toughness as shown in Table I [5, 6]. During sintering at 1500–1600 °C in air, plate-like crystals of LBA grow in Ce-TZP matrix (Fig. 1), leading to the improvement of the mechanical properties. Although the microstructure development was found to improve the mechanical properties, the formation process of the anisotropic LBA crystals in the Ce-TZP matrix has not been revealed.

This paper describes the formation process of the anisotropic LBA crystals during heat treatments. The effect of the particle size of raw starting Al_2O_3 powder is also demonstrated and discussed in relation to the microstructure development.

2. Experimental Procedure

2.1. Preparation of starting powder mixtures and green compacts

Commercially available Ce-TZP (12 mol % CeO_2–ZrO_2; Tosoh Co., TZ-12CE) powders, Al_2O_3 and lanthanum oxalate (reagent grade, $La_2(C_2O_4)_3 9H_2O$ powders; Wako Pure Chemical Industries, Ltd) were used as starting materials. Three types of α-Al_2O_3 powders (reagent grade, average particle size 0.4 μm (Sumitomo Chemical Industries Co., AKP-30), 3.6 and 10.3 μm (Showa Denko Co.) and γ-Al_2O_3 (Asahi Aluminium Co.) were selected in order to examine the effect of the particle size of the starting Al_2O_3 powder on the morphology of the grown LBA crystals. The appropriate amount of the starting powder materials was mixed with ethanol in a plastic ball mill for 24 h. The composition used in this experiment was adjusted to be 85 wt % Ce-TZP/15 wt % LBA after firing, which

0022–2461

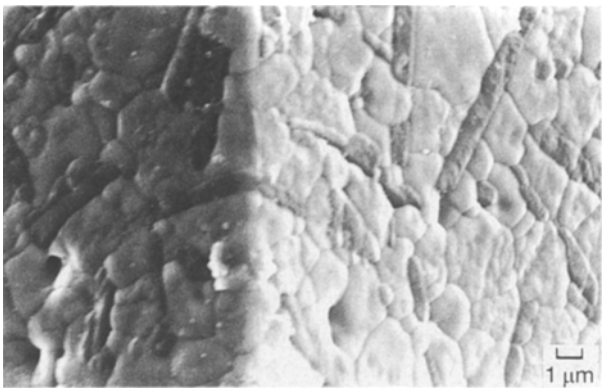

Figure 1 Scanning electron micrograph of plate-like LBA crystals grown in the Ce-TZP matrix.

TABLE I Mechanical properties of Ce-TZP based ceramics.

	Al_2O_3 (wt %)	LBA (wt %)	Fracture strength (MPa)	Fracture toughness (MPa $m^{1/2}$)
12Ce-TZP	0	0	650	8.1
12Ce-TZP/Al_2O_3	20	0	930	6.4
12Ce-TZP/Al_2O_3/LBA	15	5	910	11.2

was the proper composition to achieve the best mechanical properties [6]. After drying the slurry at 110 °C, the mixture powder was sieved through a 145-mesh screen. Ce-TZP/Al_2O_3, Ce-TZP/lanthanum oxalate and Ce-TZP/$LaAlO_3$ mixture powders are also prepared in the same manner in order to investigate the formation process of LBA. The $LaAlO_3$ powder was prepared in advance by the solid-state reaction of lanthanum oxalate with Al_2O_3 mixture powder.

The mixed powders were die-pressed under 59 MPa. To examine the growth process of the LBA crystals, green compacts of a duplex structure were also prepared as shown in Fig. 2. First, the inner part was die-pressed (e.g. Ce-TZP/lanthanum oxalate mixture powder) and pre-fired at 1600 °C to form a disc

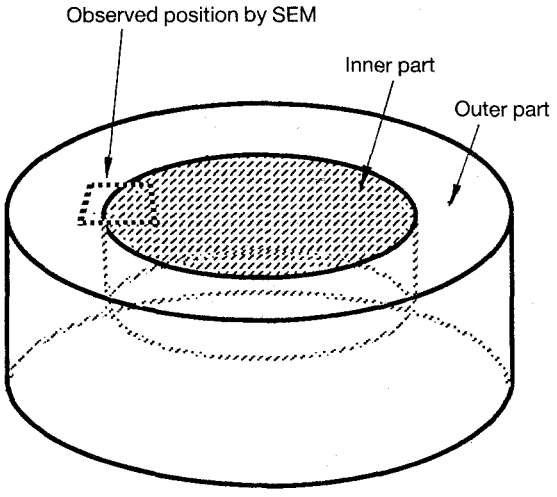

Figure 2 Assembly of samples: inner part, Ce-TZP/$LaAlO_3$ or La_2O_3 (lanthanum oxalate); outer part, ZrO_2/Al_2O_3. (- - - - -) Area observed by SEM.

specimen. The specimen was placed in a die of diameter larger than that of the disc specimen, and subsequently the outer part (e.g. ZrO_2/Al_2O_3 mixture) powder was fed into a die and press-formed again to give a duplex cylindrical compact.

The compacts were fired at a heating rate of 10 °C min^{-1} to the desired temperature in air and kept at that temperature for up to 8 h. The compacts were then allowed to furnace-cool.

2.2. Characterization

Characterizations were performed on the interior portion of the compacts. The surface layer of as-fired compacts was removed by grinding and finished with 1 μm diamond paste prior to evaluation of the properties.

The crystalline phases were identified by X-ray diffractometry (XRD) using CuK_α radiation at 30 kV and 15 mA with a graphite monochromater and by Raman spectroscopy.

Microstructure of the compacts was examined with a scanning electron microscope (SEM). The finished surfaces of the compacts were thermally etched at the temperature of 50 °C lower than that of the sintering temperature prior to observation.

3. Results and discussion

3.1. Formation of LBA crystal in Ce-TZP matrix

3.1.1. Reaction process

Ce-TZP, α-alumina (0.4 μm) and lanthanum oxalate were mixed and compacted to the nominal composition of 85 wt % Ce-TZP/15 wt % LBA. Fig. 3 shows the XRD profiles of the specimens heat-treated at 800, 1000, 1200, 1500 and 1600 °C for 4 h in air. The formation of $LaAlO_3$ was completed at temperatures above 1200 °C within 4 h. Ropp and Carroll [7] reported that the formation of $LaAlO_3$ was completed at 800 °C by prolonging the time to 24 h. The crystalline phase of $La_2Zr_2O_7$ was detected between 800 °C and 1500 °C. The formation of LBA began above 1500 °C. The complete formation of LBA was achieved at 1600 °C within 1 h. The temperature of 1600 °C was chosen as the fixed heat-treatment temperature to study the formation mechanism of LBA. Godina and Keler [8] reported that the solid-state formation of LBA by the reaction between La_2O_3 and Al_2O_3 progressed through two stages.

$$La_2O_3 + Al_2O_3 \rightarrow 2LaAl_2O_3\,(LA) \quad (1)$$

$$LaAlO_3 + 5Al_2O_3 \rightarrow LaAl_{11}O_{18}\,(LBA) \quad (2)$$

In the Ce-TZP matrix, La^{3+} reacts with the ZrO_2 matrix to form $La_2Zr_2O_7$ and diffuses through the matrix. Then, La^{3+} reacts with Al_2O_3 to form LA. The LA reacts further with Al_2O_3 to form LBA. It was found that the formation of LBA proceeded through the following stages

$$La_2O_3 + 2ZrO_2 \rightarrow La_2Zr_2O_7 \quad (3)$$

$$La_2Zr_2O_7 + Al_2O_3 \rightarrow 2LaAlO_3 + 2ZrO_2 \quad (4)$$

$$LaAlO_3 + 5Al_2O_3 \rightarrow LaAl_{11}O_{18}\,(LBA) \quad (5)$$

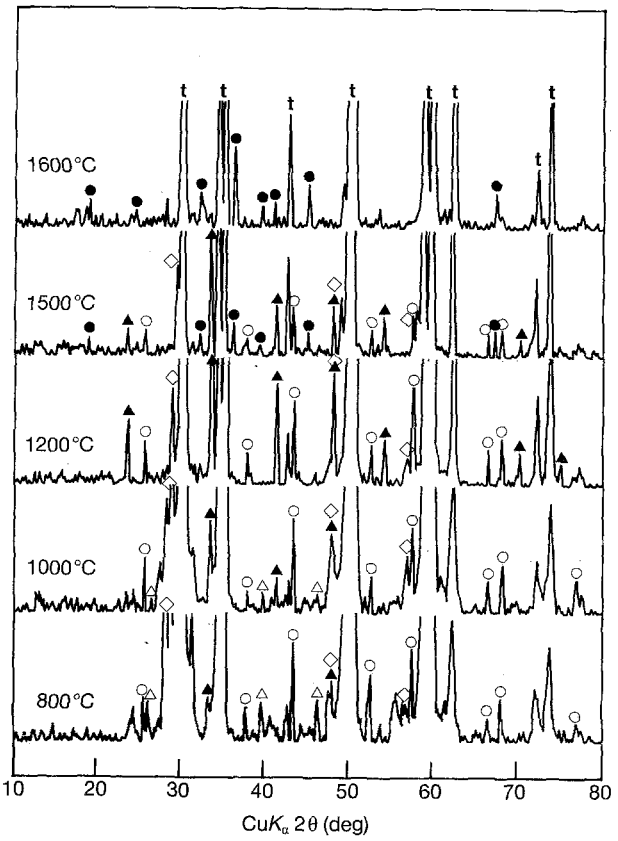

Figure 3 Temperature dependence of crystalline phase of Ce-TZP/LBA composite. (The starting compact consists of Ce-TZP, α-Al_2O_3 (0.4 μm) and lanthanum oxalate.) (●) $LaAl_{11}O_{18}$ (LBA), (▲) $LaAlO_3$ (LA), (○) α-Al_2O_3, (△) La_2O_3, (◇) $La_2Zr_2O_7$; (t) t-ZrO_2.

3.1.2. Reaction mechanism

In order to investigate the formation process of anisotropic LBA crystals during the heat treatment, the samples were assembled as shown in Fig. 2. Fig. 4 shows the microstructure of the duplex-type compact (the inner part is Ce-TZP/$LaAlO_3$ mixture and the outer is Ce-TZP/Al_2O_3 mixture) heat treated at 1600 °C for 4 h. The observed position is indicated schematically with the dashed line in Fig. 2. The left side of the figure (Part A) is Ce-TZP/Al_2O_3 (molar ratio, 1/1) and the right (Part B) is Ce-TZP/$LaAlO_3$ (molar ratio, 1/1). XRD examinations revealed that LBA crystal was formed at the interface of the two parts. The dark and bright contrasts in the scanning electron micrograph are LBA crystals and ZrO_2 grains, respectively. The arrow in the figure displays the interface of the initial green compact. Anisotropic LBA crystals are found to grow at the interface to the interior of the Ce-TZP/Al_2O_3 part, indicating that the $LaAlO_3$ grains in the Ce-TZP/$LaAlO_3$ part appear to decompose at high temperature (e.g. 1600 °C) and the resulting La^{3+} ions diffuse to the Ce-TZP/Al_2O_3 part to form LBA. The intermediate phase of the diffusion process is confirmed to be $La_2Zr_2O_7$. This result indicates that Equation 4 is irreversible. Ropp and Carroll [7] suggested two possible diffusion mechanisms for the formation of LBA by the reaction

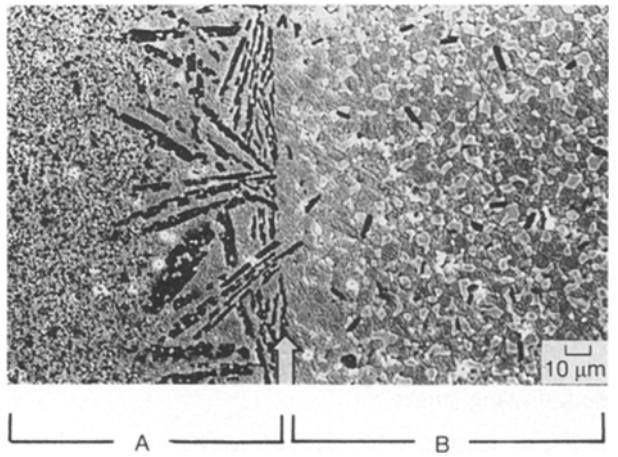

Figure 4 Scanning electron micrograph of duplex-type sintered compact fired at 1600° C for 4 h. (The inner part is Ce-TZP/$LaAlO_3$ mixture and the outer part is Ce-TZP/Al_2O_3 mixture.)

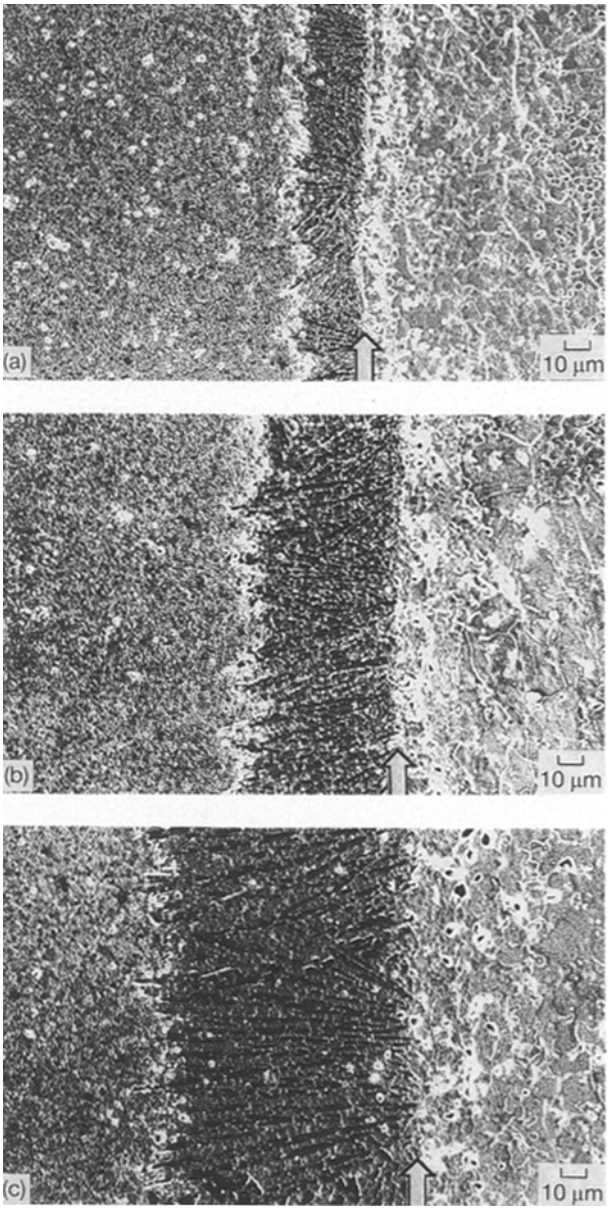

Figure 5 Change of the interfaces of a duplex-type compact with time at 1600 °C. (The inner part is Ce-TZP/La_2O_3 (lanthanum oxalate) mixture and the outer part is Ce-TZP/Al_2O_3 mixture.) (a) 0.5 h, (b) 1 h, (c) 4 h.

between $LaAlO_3$ and Al_2O_3, namely either Al^{3+} diffusion mechanism or La^{3+} diffusion mechanism. According to the mode of formation of LBA crystals in Ce-TZP matrix, the rate of diffusion of Al^{3+} is lower than that of La^{3+}. Another interesting observation in the figure is that anisotropic small crystals about 10 μm in length also exist in the $ZrO_2/LaAlO_3$ part. These are formed by the reaction between La^{3+} and excess Al_2O_3 remaining after the decomposition of $LaAlO_3$ and the following diffusion of La^{3+} to the Ce-TZP/Al_2O_3 part.

As a model for the formation of Ce-TZP/LBA composite, the Ce-TZP/Al_2O_3 compact was joined to the Ce-TZP/lanthanum oxalate compact, and the specimen was heat treated to observe the interface. Fig. 5 shows the change of the microstructure at the joining interface with heat-treatment time (0.5, 1, 4 h). The left side of the figure is the area of ZrO_2/Al_2O_3 (molar ratio, 1/1) and the right is ZrO_2/lanthanum oxalate (molar ratio, 1/1). The arrows in the figures indicate the interface of the initial green compact. In the ZrO_2/lanthanum oxalate part, the formation of $La_2Zr_2O_7$ was observed by XRD. LBA crystals were formed near the interface of the Ce-TZP/Al_2O_3 part. These anisotropic LBA crystals grew from the interface to the inner region of the Ce-ZrO_2/Al_2O_3 part and increased in length with prolonged holding time. Fig. 6 shows the fine-focus X-ray diffraction profiles of the parts indicated in Fig. 7. The results reveal that the formation of LBA takes place in the Ce-TZP/Al_2O_3 part, which was also identified by the Raman spectroscopy. This phenomenon also indicates that the diffusion of La^{3+} leads to the formation of the LBA crystals. The amount of growth of LBA grains seems to be dependent on the heating and cooling stages.

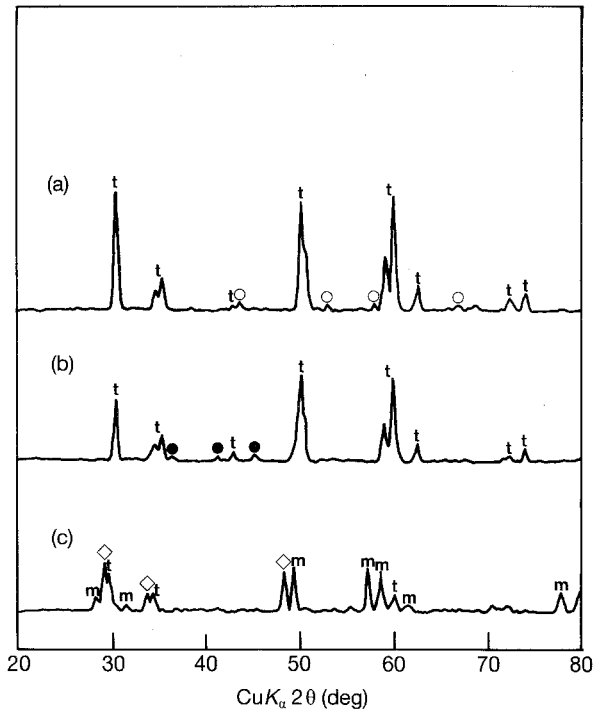

Figure 6 Fine-focus X-ray diffraction profiles of a duplex cylindrical compact fired at 1600 °C for 4 h. The analysed points are indicated schematically in Fig. 7. (The inner part is Ce-TZP/La_2O_3 (lanthanum oxalate) mixture and the outer part is Ce-TZP/Al_2O_3 mixture.) (●) LBA; (○) α-Al_2O_3; (t) t-ZrO_2; (m) m-ZrO_2; (◇) $La_2Zr_2O_7$.

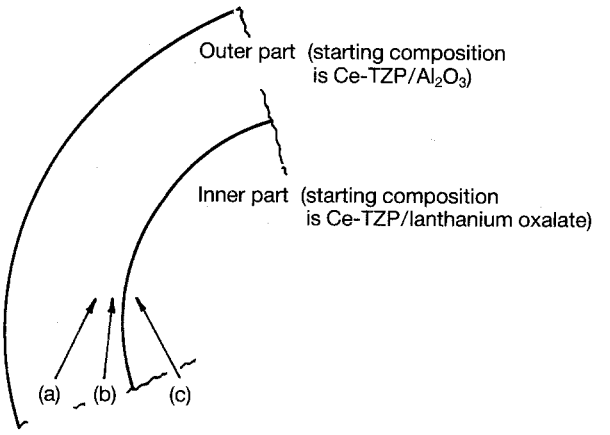

Figure 7 Schematic illustration of the points analysed by fine-focus XRD.

3.2. Effects of starting Al_2O_3 particles on morphology of LBA

Fig. 8 shows scanning electron micrographs of the sintered specimen at 1600 °C from Ce-TZP–lanthanum oxalate with the corresponding starting Al_2O_3 particles of different sizes (0.4, 3.6, 10.3 μm). It was observed that the average particle size of the starting Al_2O_3 powder has a predominant effect on the control of morphology of the grown LBA crystals. Anisotropic plate-like LBA crystals grew when the submicrometre size Al_2O_3 (0.4 μm) was used (Fig. 8a). In contrast, when 3.6 μm Al_2O_3 were employed, the LBA crystals which are indicated as black contrast in Fig. 8b appeared to be granular agglomerates with a similar size to that of the raw Al_2O_3 particles. A similar phenomenon was confirmed in the specimen with 10.3 μm Al_2O_3 raw powder (Fig. 8c). Fig. 9 shows a magnified photograph of the LBA crystals in Fig. 8c. It is indicated that the black contrast of LBA is a conglomerate which consists of some small plate-like crystals.

Fig. 10 shows the microstructure of sintered compacts using 0.4 or 3.6 μm Al_2O_3 powders fired at 1400 °C. The crystalline phases of both specimens consist of t-ZrO_2, $La_2Zr_2O_7$, $LaAlO_3$ and Al_2O_3 without any LBA crystal at this temperature. The dark region in the photographs is $LaAlO_3$ or Al_2O_3 grains. It is recognized that the $LaAlO_3$ grains were not anisotropic even in the specimen using 0.4 μm Al_2O_3 powder at this temperature. When the submicrometre size Al_2O_3 (0.4 μm) is used, the $LaAlO_3$ particles are larger than the raw powders (Fig. 10a). When the 3.6 or 10.3 μm Al_2O_3 grains are used, the grain size of $LaAlO_3$ formed is similar to that of the corresponding starting raw Al_2O_3 powders (Fig. 10b).

The formation process of LBA is schematically shown in Fig. 11 in connection with the raw Al_2O_3 particle size and the sintering stages. When 0.4 μm Al_2O_3 is employed, the Al_2O_3 particles gather through the grain growth of the matrix and react with

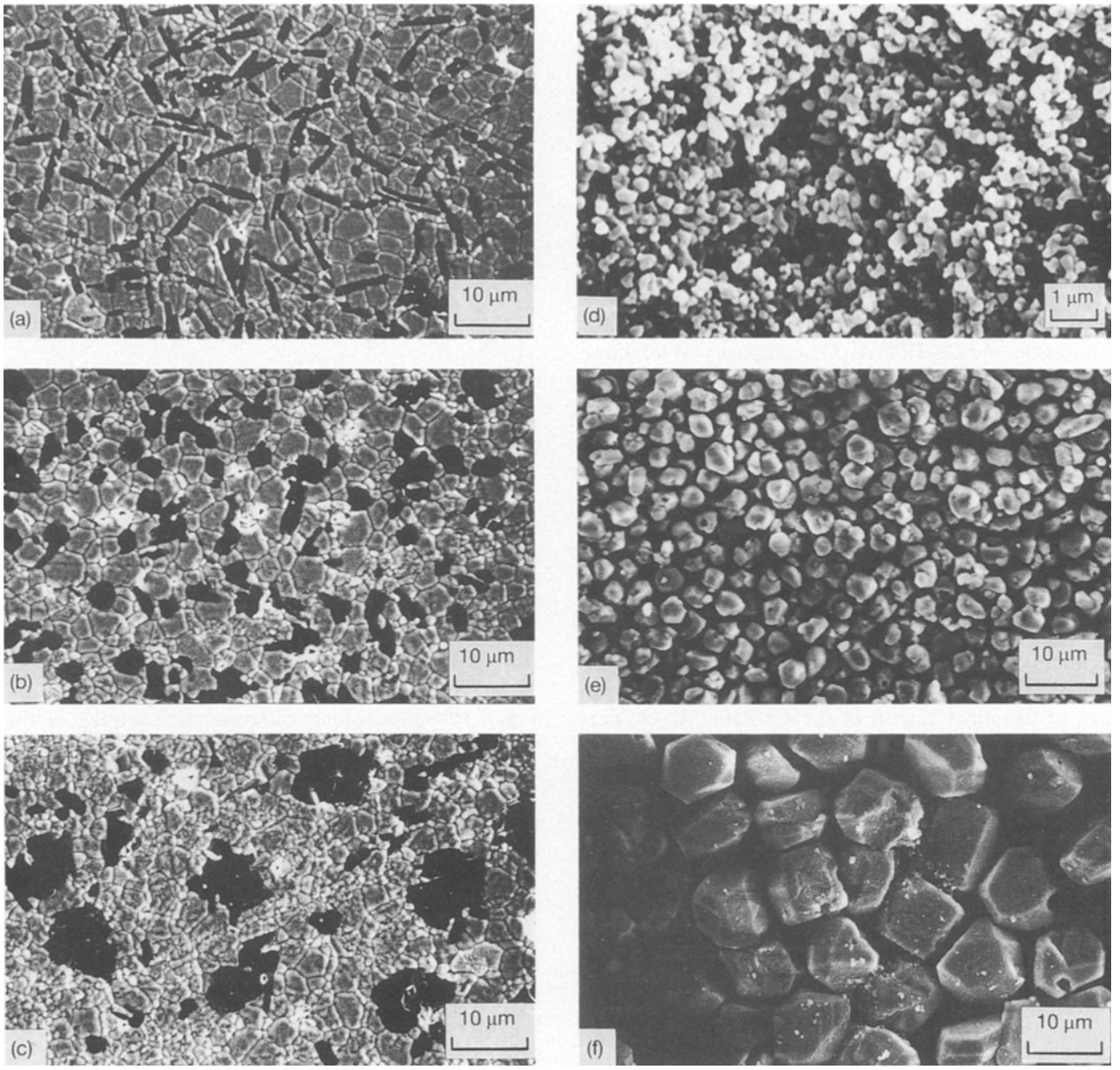

Figure 8 Scanning electron micrographs of Ce-TZP/LBA composites from (a–c) Ce-TZP–Al_2O_3–lanthanum oxalate fired at 1600 °C and (d–f) the corresponding Al_2O_3 powders: (a) 0.4 μm, (b) 3.6 μm, (c) 10.3 μm.

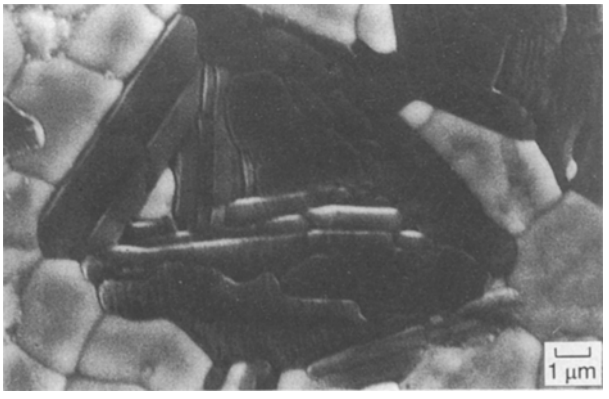

Figure 9 Scanning electron micrograph of magnified conglomerate of LBA shown in Fig. 5c.

each other to give larger crystals, and the LA crystals produced by the reaction between Al_2O_3 and La^{3+} are around 1–2 μm diameter (Fig. 11b). Furthermore, the LA crystals grow larger as the grain growth of the matrix advances. At a firing temperature of 1600 °C, the LA crystals react further with Al_2O_3 to give 10 μm LBA crystals (Fig. 11c). The sintering process of Ce-TZP matrix and the particle size of Al_2O_3 (0.4 μm) easily promote the growth of 10 μm size anisotropic LBA crystals. On the other hand, large size Al_2O_3 (3.6 or 10.3 μm) grains do not give well-dispersed LBA crystals. In this case, the particle size and morphology of LA crystals which formed at the intermediate stages of LBA formation do not change remarkably from the raw (3.6 or 10.3 μm size) Al_2O_3 particles regardless of the grain growth of the matrix (Fig. 11e). Then, the LBA crystals grow as conglomerates at the position where raw Al_2O_3 particles or LA existed.

Fig. 12 shows Ce-TZP/LBA composites prepared at 1600 °C for 1 and 4 h, respectively. The grain size of LBA crystals has not changed in relation to the firing time. The XRD analysis of these specimens indicated that Ce-TZP and LBA crystal were produced and no other phase (e.g. Al_2O_3, $LaAlO_3$) remained at 1600 °C

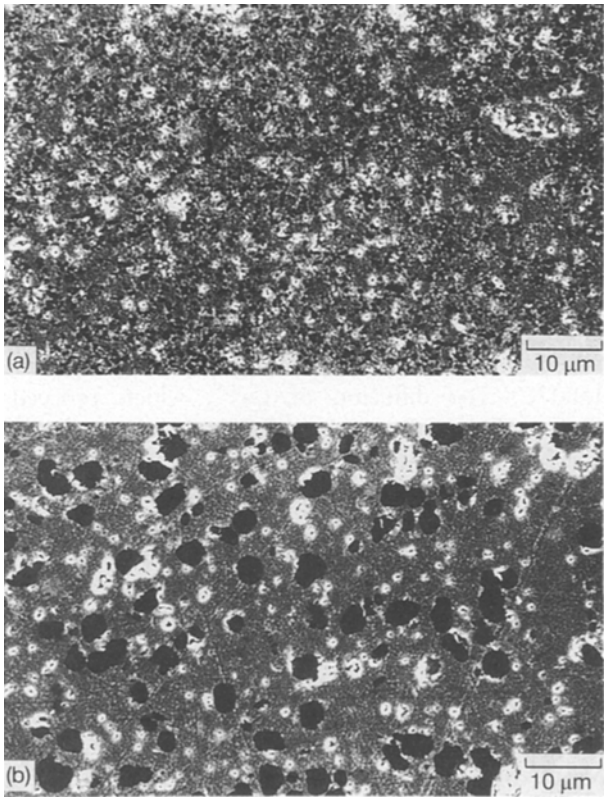

Figure 10 Scanning electron micrograph of sintered products formed from Ce-TZP–Al_2O_3–lanthanum oxalate at 1400 °C using (a) 0.4 μm or (b) 3.6 μm Al_2O_3.

for 1 h, showing that the formation of LBA has been completed within that time. Once the formation of LBA is finished, the LBA crystals are quite stable and do not decompose to diffuse into larger LBA grains, which reflects the independence of the size of LBA crystals with the firing time, as shown in Fig. 12. Although the ZrO_2 matrix shows grain growth with firing time, the morphology of LBA crystals has not changed. These facts indicate that the early stage of the firing process (the initial sintering of ZrO_2) is very important for control of the morphology of LBA grains.

Fig. 13 shows the microstructure of Ce-TZP/LBA composite which was fired using γ-Al_2O_3 grains as raw particles. The formation of small size (~ 4 μm) LBA grains was obvious. In this case the transformation of γ-Al_2O_3 to α-Al_2O_3 which took place at 1200 °C enhanced the reaction with La_2O_3 to create a higher number of nuclei of LBA crystals, leading to the formation of the small-sized LBA crystals in the Ce-TZP matrix, as expected by the van't Hoff's criterion. Although the reaction process for producing LBA is the same as that in the case of α-Al_2O_3 particles as starting raw powders, the reaction temperature was lowered about 100 °C by using γ-Al_2O_3 particles. In this case, γ-Al_2O_3 grains are so small and reactive that LBA embryos were formed in high density at many points compared with the specimen using 0.4 μm α-Al_2O_3 grains (Fig. 8a). Because LBA crystals were formed in higher density, each LBA crystal remained small and homogeneously dispersed. This highly dense nucleation is attributable to the less-sufficient grain growth of LBA crystals to increase the toughness, as shown in Table I. It is quite clear that the morphology of LBA can be controlled by employing an adequate size of raw Al_2O_3 particles, and the optimum particle

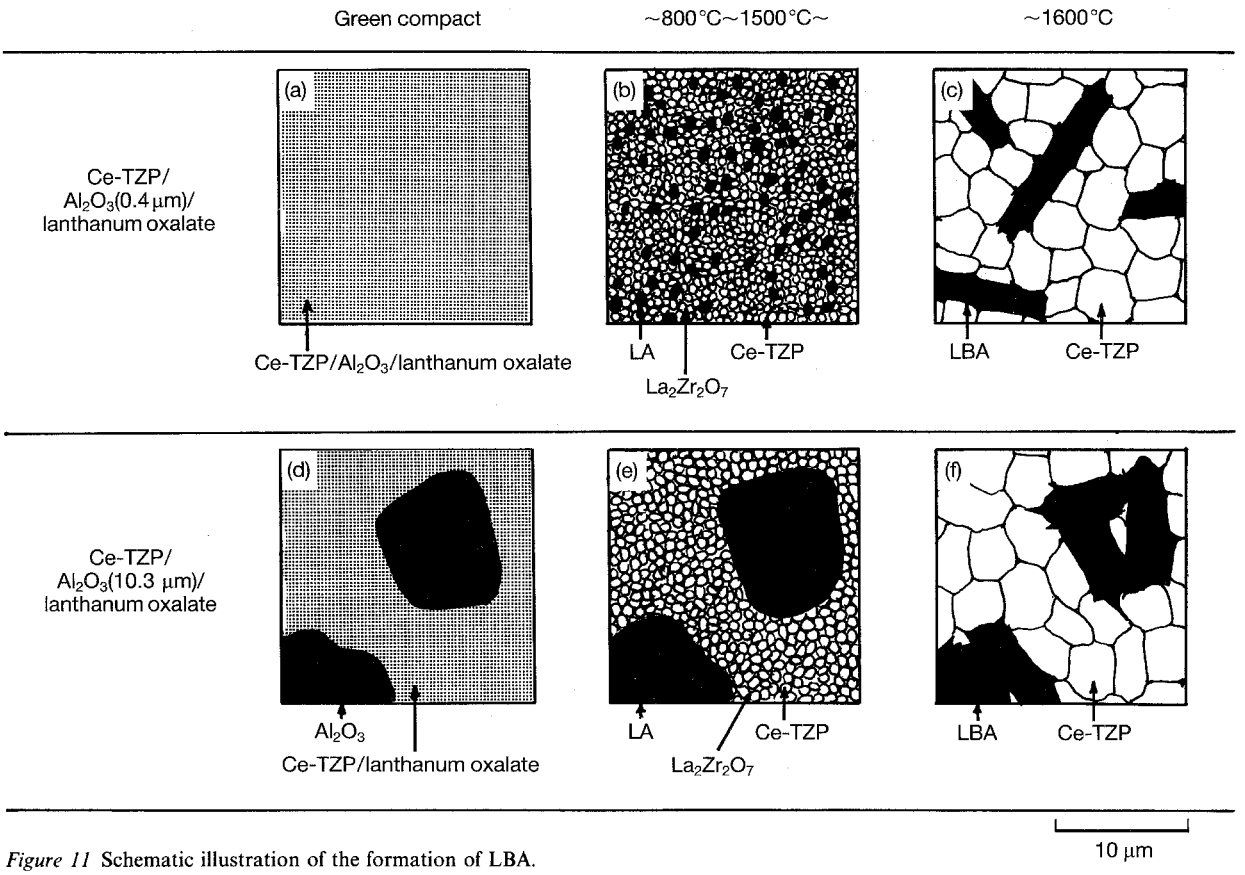

Figure 11 Schematic illustration of the formation of LBA.

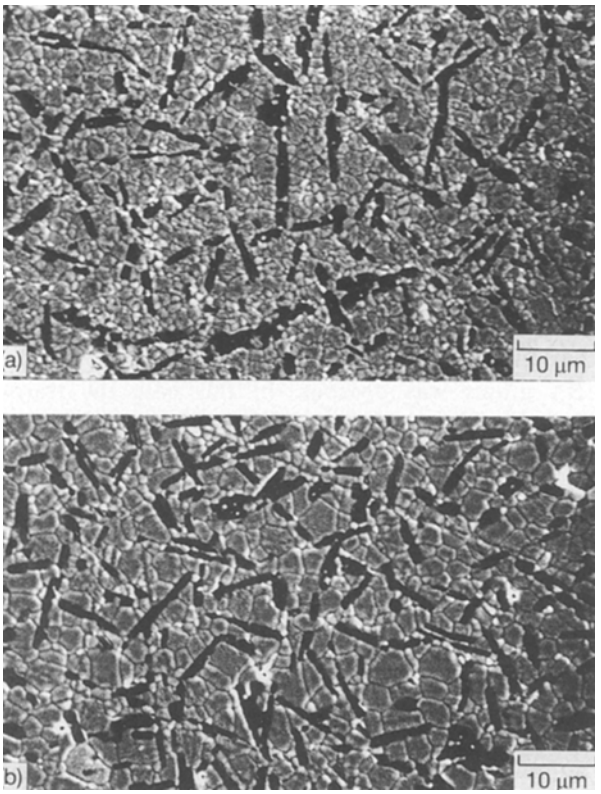

Figure 12 Scanning electron micrograph of Ce-TZP/LBA composite from Ce-TZP–Al_2O_3– lanthanum oxalate at 1600 °C for (a) 1 h and (b) 4 h.

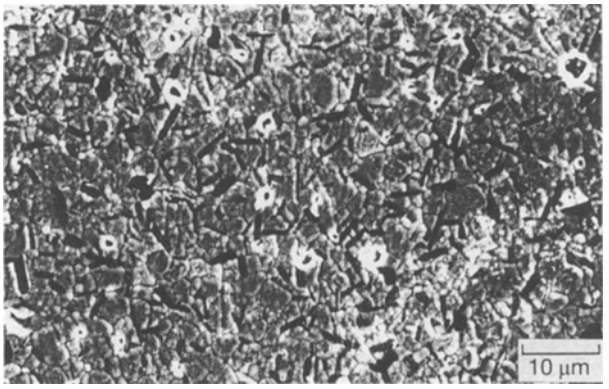

Figure 13 SEM of Ce-TZP/LBA composite using γ-Al_2O_3 as raw material.

size of the Al_2O_3 grains for the formation of anisotropic plate-like LBA crystals is found to be around the submicrometre level. The plate-like LBA crystals formed *in situ* in Ce-TZP matrix during sintering act as dispersed particles to increase the strength and the toughness of the Ce-TZP ceramics.

4. Conclusion

The formation of LBA by the reaction between La_2O_3 and Al_2O_3 in Ce-TZP matrix proceeds through the intermediate formation of $La_2Zr_2O_7$ and $LaAlO_3$. The formation of $La_2Zr_2O_7$ is detected between 800 and 1500 °C. $LaAlO_3$ starts to form below 1400 °C, followed by the formation of LBA with Al_2O_3 above 1500 °C. The diffusion of La^{3+}, which proceeds through $La_2Zr_2O_7$ phase, is faster than that of Al^{3+} and becomes a dominant factor in the formation and control of the morphology of LBA particles. The particle size of starting Al_2O_3 grains plays an important role in controlling the morphology of LBA crystals. The anisotropic, plate-like LBA crystals were formed successfully in Ce-TZP matrix using adequate Al_2O_3 grains of submicrometre size (0.4 μm) at 1600 °C, which lead to the improvement in the toughness and strength of Ce-TZP ceramics. Large size (3.6, 10.3 μm) Al_2O_3 particles yield conglomerates which consist of several LBA crystals. This result indicates that the morphology of LBA in the Ce-TZP matrix is dependent on the particle size of the starting Al_2O_3 and the sintering process of the matrix.

References

1. T. SATO and M. SHIMADA, *J. Am. Ceram. Soc.* **67** (1984) C-212.
2. K. TSUKUMA, *Am. Ceram. Soc. Bull.* **65** (1986) 1386.
3. T. SATO and M. SHIMADA *ibid* **64** (1985) 1382.
4. K. TSUKUMA, T. TAKAHASHI and M. SHIOMI, in "Advances In Ceramics", Vol. 24, edited by N. Claussen, M. Ruhel and A. H. Heuer (The American Ceramic Society, Columbus, OH, 1988) p. 721.
5. T. FUJII, H. MURAGAKI, H. HATANO and S. HIRANO, *Ceram. Trans.* **22** (1991) 693.
6. T. FUJII, H. MURAGAKI, H. HATANO and S. HIRANO. *Mater. Res. Soc. Symp. Proc.* **274** (1992) 141.
7. R. C. ROPP and B. CARROLL, *J. Am. Ceram. Soc.* **63** (1980) 416.
8. N. A. GODINA and E. K. KELER, *Izv. Akad. Nauk SSSR, Ser. Khim.*(1) (1966) 24.

Received 15 April
and accepted 3 June 1993